AD-A156 724 DESIGN AND CALIBRATION OF A FLAT-FLAME BURNER USING LINE REVERSAL TECHNIQUES(U) DEFENCE RESEARCH ESTABLISHMENT OTTAWA (ONTARIO) D R SNELLING ET AL. 1/1

UNCLASSIFIED APR 85 DREO-TN-85-4 F/G 21/2 NL

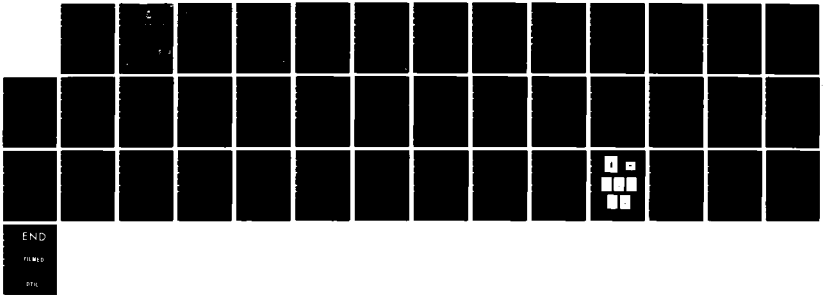

END

FILMED

DTIC

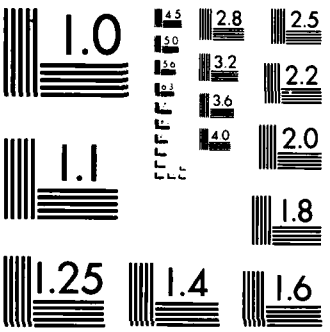

National Defence / Défense nationale

DESIGN AND CALIBRATION OF A FLAT-FLAME BURNER USING LINE REVERSAL TECHNIQUES

by

D.R. Snelling and M. Fischer

DEFENCE RESEARCH ESTABLISHMENT OTTAWA
TECHNICAL NOTE 85-4

Canada

April 1985
Ottawa

National Defence / Défense nationale

DESIGN AND CALIBRATION OF A FLAT-FLAME BURNER USING LINE REVERSAL TECHNIQUES

by

D.R. Snelling and M. Fischer
Energy Systems Section
Energy Conversion Division

DEFENCE RESEARCH ESTABLISHMENT OTTAWA
TECHNICAL NOTE 85-4

PCN
25B10

April 1985
Ottawa

ABSTRACT

A premixed methane/air flat-flame burner is described. The burner was designed to have a central flame which could be seeded with sodium, and an annular guard flame which ensured a flat temperature profile in the seeded region.

The burner produced a well behaved flat flame for linear gas velocities of 20 to 30 cm/s and air to fuel ratios within 15% of stoichiometric. The temperature distribution in the flame was measured for a range of operating conditions using the sodium line-reversal technique. The temperatures measured were within the range 2000 - 2100 K, slightly lower than the adiabatic methane/air flame temperature. This burner will be used as a calibration tool in the development of CARS (Coherent anti-Stokes Raman spectroscopy).

RÉSUMÉ

On décrit un brûleur produisant une flamme plate alimentée par un mélange méthane/air pré-mélangé. Le brûleur est conçu de façon à produire une flamme centrale dans laquelle il est possible d'injecter du sodium, et une flamme annulaire de protection assurant une température constante dans la zone d'injection.

Le brûleur produit une flamme plate qui se comporte bien à des vitesses linéaires du gaz de 20 à 30 cm/s et à des rapports air/carburant s'écartant de moins de 15 p. cent du rapport stoechiométrique. On a mesuré la distribution des températures dans la flamme pour une gamme de conditions d'utilisation, en employant la technique d'inversion de la raie de sodium. Les températures mesurées étaient comprises entre 2000 et 2100 K, c'est-à-dire qu'elles étaient légèrement inférieures à la température adiabatique d'une flamme méthane/air. Le brûleur sera utilisé à des fins d'étalonnage au cours de la mise au point de la spectroscopie Raman anti-Stokes en lumière cohérente.

TABLE OF CONTENTS

1.0 INTRODUCTION

Coherent anti-Stokes Raman spectroscopy (CARS) is an optical technique capable of providing measurements of temperature and major species concentration in practical combustion environments. A broadband CARS system was developed at the Defence Research Establishment Ottawa (DREO) capable of obtaining CARS spectra from a single laser pulse. Flame temperatures are readily obtained by comparing experimental N_2 CARS spectra to theoretical CARS spectra calculated for a range of temperatures. The CARS system, which has good spatial resolution (typically the measurement volume is a cylinder 2 to 3 mm long and 0.1 mm diameter) and temporal resolution (10 ns), was designed to be applicable to turbulent combustion phenomena in practical combustion environments.

To compare CARS temperature measurements with those obtained from more conventional and better established techniques it was decided to build a premixed air/fuel burner which would be non-turbulent and would provide a well controlled, constant temperature, flame. A premixed methane/air flat-flame burner (1) is such a source.

A spectroscopic line-reversal technique was chosen to measure temperature in the burner. This technique is non-intrusive and can be used to measure temperatures well above those accessible to thermocouples and other probe techniques. The (sodium) line-reversal technique used is based on the comparison of radiation from a background source of known temperature to that from (sodium) emission in the flame. The temperature determined by this method is a line of sight average over the part of the flame seen by the optical system. In the presence of significant thermal boundary layers, or other inhomogeneities, care must be taken in the interpretation of results. In the design of the burner for this investigation, steps were taken to reduce high thermal gradients in the portion of the flame over which the temperature is measured (i.e., the sodium seeded portion).

In this report we describe the design, calibration and operation of a flat-flame burner and the theory, design, and operation of a Na line-reversal temperature measurement system. Measurements of the temperature distributions in the burner under various conditions of flow rate and equivalence ratio are presented and discussed.

2.0 THEORY

2.1 Temperature Measurements by Line Reversal

The line reversal method involves trans-illuminating the flame with a calibrated background source (usually a tungsten strip filament lamp). The flame is seeded with an atom having an appropriate emission line e.g., sodium. Radiation from the background source, together with

radiation emitted by the sodium atoms are imaged on the entrance slit of a monochromator. The detected output from the monochromator as the latter is scanned slowly across the emission line (589. nm for Na) is recorded. If the lamp brightness temperature, T_L, is lower than the flame temperature, T_F, the sodium radiation is seen as an emission peak against the continuum background of the lamp, whereas if $T_L > T_F$, the line appears as an absorption dip in the continuum. If the lamp current is adjusted until $T_L = T_F$ the line is invisible against the background.

The power flux, W, of blackbody radiation across an area δA and in a solid angle $\delta\Omega$ and a wavelength interval $\delta\lambda$ is:

$$W = L^{\circ}_{\lambda} \, \delta A \, . \, \delta\Omega \, . \, \delta\lambda$$

where the black body spectral radiance L°_{λ} is given by Planck's equation:

$$L^{\circ}_{\lambda} = \frac{C_1}{\lambda^5 \, [\exp \, (C_2/\lambda T)]-1} \qquad (1)$$

Where, $C_1 = 1.1909 \times 10^{-16}$ watt m^2 steradian^{-1}
$C_2 = 1.4380 \times 10^{-2}$ m K.

The increase in spectral radiance dL_λ across a region dx of a medium is:

$$dL_\lambda = e_\lambda \, dx - \alpha_\lambda \, L_\lambda \, dx \qquad (2)$$

where e_λ is the spectral volumetric radiant intensity of the gas (watts/m^4 - steradian) and α_λ is the spectral absorption coefficient (m^{-1}).

The method has its theoretical basis in Kirchoff's law which for gases in local thermodynamic equilibrium is:

$$e_\lambda = \alpha_\lambda \, L^{\circ}_{\lambda} \, (T_F) \qquad (3)$$

where T_F is the flame temperature.

Thus from equations 2 and 3 we have:

$$\frac{dL_\lambda}{dx} = \alpha_\lambda L^{\circ}_{\lambda} \, (T_F) - \alpha_\lambda L_\lambda \qquad (4)$$

where α_λ and $L^{\circ}_{\lambda} \, (T_F)$ are functions of λ and x since temperature and composition can vary throughout the flame. Equation 4 can be integrated across a flame extending from x = 0 to x = ℓ to give:

$$L_\lambda(\ell) = \exp - \tau_\lambda(\ell) \int_0^\ell \alpha_\lambda(x)\, L^\circ_\lambda(x) \exp \tau_\lambda(x)\, dx + L_\lambda(o) \exp - \tau_\lambda(\ell) \quad (5)$$

where the optical depth $\tau_\lambda(\ell)$ is defined by

$$\tau_\lambda(\ell) = \int_0^\ell \alpha_\lambda(x)\, dx \quad (6)$$

(With regard to the integration of equation 4 it should be noted that it is of the form

$$\frac{dy}{dx} + y\, P(x) = Q(x)$$

where $P(x) = \alpha_\lambda$ and $Q(x) = \alpha_\lambda(x)\, L^\circ_\lambda(x)$. The integrating factor for this equation is $\exp - \int P(x)\, dx$ and its integral for is

$$y = \left[\exp - \int P(x)\, dx\right] \left[Q(x) \exp \left(\int P(x)\, dx\right) \right] + C.)$$

The first term in equation 5 represents the radiation emitted by the flame that reaches $x = \ell$, while the second term is the radiation reaching $x = \ell$ from the radiation ($L_\lambda(o)$) incident on the flame at $x=0$. For a flame of uniform composition and temperature α_λ and L°_λ are no longer a function of x and equation 5 simplifies to:

$$L_\lambda(\ell) = \left[1 - \exp - \tau_\lambda(\ell)\right] L^\circ_\lambda(T_F) + \left[\exp - \tau_\lambda(\ell)\right] L_\lambda(o)(T_L) \quad (7)$$

The radiation incident on the flame at x=o ($L_\lambda(o)(T_L)$) is assumed to be from a tungsten filament lamp of brightness temperature T_L.

The brightness temperature $T_L(\lambda,T)$ of a non blackbody surface is defined as the temperature of a blackbody which, at a specified λ and T, would give the same spectral radiance as the surface, i.e.

$$L^\circ_\lambda(T_L) = \varepsilon(\lambda,T)\, L_\lambda(T) \quad (8)$$

where ε is the surface emissivity.

T_L is then always less than the true temperature T of the surface and for tungsten in the λ, T range of interest, is typically ~200 K lower. Since ε decreases with λ and T, the difference $T-T_L$ clearly increases with λ and T.

From equation 7 it can be seen that when the flame is optically thick i.e., $\tau_\lambda(\ell) \gg 1$, then $L_\lambda(\ell)$ is primarily due to sodium radiation which is originating from regions close to $x = \ell$. (Heavy seeding of the flame with sodium will increase α_λ, particularly at the centre of the sodium D-line, resulting in an optically thick flame.) When the flame is optically thin ($\tau_\lambda(\ell) \ll 1$), e.g. with light seeding or remote from the centre of the sodium D-line, then the flame contributes little to $L_\lambda(\ell)$ and the lamp radiation $L^\circ_\lambda(T_L)$ is transmitted with very little attenuation.

For a uniform flame and $T_L = T_F$ and equation 7 reduces to

$$L_\lambda(\ell) = L^o_\lambda\,(T_F) = L_\lambda(o)\;(T_L) \qquad (9)$$

It should be noted that this line reversal condition applies simultaneously at all wavelengths. Line reversal occurs as T_L is increased through the value of T_F. The line becomes 'invisible' against the background in a spectral display, reversing from an emission peak to an absorption dip against the continuum background. When no peak or dip is observed the temperatures T_L and T_F are equal.

The signal level V at the monochromator output is given by:

$$V = L^o_\lambda(T_F)\;[1 - \exp - \tau_\lambda(\ell)]\;F_1.S.\delta A.\delta\Omega.\delta\lambda + [\exp - \tau_\lambda(\ell)]$$

$$L^o_\lambda(T_L)\;F_1.F_2.S.\delta A_1.\delta\Omega_1.\delta\lambda \qquad (10)$$

$\delta\lambda$, the effective pass band of the monochromator, is determined by the entrance slit and the dispersion. δA is the effective area of the flame that is imaged on to the monochromator slit and $\delta\Omega$ is the solid angle over which flame radiation is collected by the monochromator. δA_1 and $\delta\Omega_1$ are the corresponding quantities for lamp radiation. F_1 is the transmission of the optics between the flame and the detector and F_2 is the transmission of the optics between the lamp filament and the flame. S is the sensitivity of the detector in Volt/watt.

In order to avoid large errors in line reversal measurements, it is essential that $\delta A.\delta\Omega = \delta A_1.\delta\Omega_1$. δA is determined by the field stop of the system and $\delta\Omega$ by the aperture stop. Physically, the above condition requires that every portion of the flame that illuminates the monochromator be trans-illuminated by radiation from the lamp.

Account must also be taken of the variation of pre-flame optical transmission (F_2). The post-flame transmission F_1 is common to both terms in equation (10) and is unimportant.

The above discussion applies to uniform flames. If the flame is non-uniform then the reversal condition, equation (9), cannot be satisfied simultaneously at all wavelengths. If a hot central core of the flame is viewed through a cooler boundary layer, then the line-reversal temperature obtained is intermediate between these two values and is a function of optical depth and hence seeding levels. In order to avoid the complex corrections which are necessary to account for boundary layer effects we have designed the burner to have a sodium seeded region of uniform temperature.

2.2 Tungsten Strip Filament Lamps

The GE 30A/6V tungsten ribbon filament lamp consists of an electrically heated thin tungsten ribbon, mounted in an evacuated glass envelope. (A calibrated GE 30A/6V lamp was used as the primary radiance standard in this work.)

The spectral radiance of the emitted radiation is given by equation (8):

where, for wavelengths and temperatures of interest the emissivity, ε, $\sim 0.4 - 0.5$ and is a function of λ and T (the true ribbon filament temperature). In addition ε may generally be a function of the angle at which the radiation is received, but this is invariably taken as normal to the surface. Also ε may depend on the purity and crystalline state of the tungsten, both of which may change as the lamp is run at high temperatures.

When a strip filament lamp is calibrated against primary standards a table of brightness temperature at 655.0 nm versus lamp current is supplied. Alternatively (and equivalently) the spectral radiance will be given as a function of lamp current. For a given current (and hence filament temperature) it can be seen from equation (8) that the brightness temperature of a lamp will be higher or lower at wavelength λ_1 different from λ depending on whether $\varepsilon(\lambda_1,T)$ is greater or less than $\varepsilon(\lambda,T)$. When sodium is used in the flame, one needs to know the brightness temperature $T_B(\lambda)$ of the lamp at the wavelength λ_1 = 589.0 nm (i.e. the stronger of the two Na D lines). This can be obtained from the calibration of the brightness temperature $T_B(\lambda)$ at the standard wavelength λ if the emissivity $\varepsilon(\lambda,T)$ is known for tungsten as a function of wavelength and the lamp filament temperature T.

The emissivity of tungsten over the ranges T = 1600-2400 K and λ = 300 to 800 nm has been determined by Larrabee(2). Using this data one can then calculate the brightness temperature for a range of filament temperatures from equations (1) and (8). This has been done(3) for three specific wavelengths 589.0, 655.0 and 766.5 nm and the results are shown in Table I. The quantity $\Delta T_B(\lambda_1)$ is the difference in brightness temperatures of the filament at wavelength λ_1 and 655 nm, the wavelength at which the lamps are calibrated.

$$\Delta T_B(\lambda_1) = T_B(\lambda_1) - T_B(655)$$

If the spectra radiance L_λ rather than brightness temperature at some wavelength $\lambda[T_B(\lambda)]$ is given then the latter can be obtained from equation (1) which, on rearranging, gives

$$T_B(\lambda) = C_2/[\lambda \, \ell n(C_1/\lambda^5 L_\lambda) + 1] \qquad (11)$$

2.3 Flat-Flame Burner

The burner used in this work is patterned on that described by Botha and Spalding(1). The flame is established above a water-cooled porous metal plate and the flame front is stabilized by heat transfer to the burner surface. If the premixed fuel/air gas stream is ignited downstream of the disk, a flame will form which will travel upstream provided the flame speed of the mixture exceeds the stream velocity. As the flame front approaches the burner surface then energy transfer to the cooled surface reduces the temperature of the burned gas with a consequent reduction in flame velocity. As a result, the flame rapidly and automatically takes up a position of equilibrium a short distance away from the disk, where it loses just enough heat to reduce the flame speed to the stream velocity. Thus a stabilized flat flame is produced.

3.0 EXPERIMENTAL

3.1 Burner Design

The requirement is for a premixed fuel/air flat flame burner with a uniform flame front. The choice of the sodium line-reversal method of temperature measurement puts restrictions on the design of the burner. Because the method results in a line-of-sight average flame temperature, the flame temperature profile must be as uniform as possible. Also, since the method is based on the absorption and emission of sodium, sodium from some source must be available in the flame. To achieve a flat flame at high flow rates, the burner surface must be cooled in some way. The centre portion of the burner must allow sodium to pass as well as the mixture of fuel and air. To avoid the effect of a large temperature gradient around the edge of the sodium seeded portion of the flame, a second unseeded flame is required to surround the seeded flame. Through this annulus of the burner will flow the same fuel/air mixture of gases as in the center, but with no sodium. To further protect the flame from atmospheric effects, a sheath of inert gas surrounding the second flame is desirable.

After some experimentation the burner design shown in Figures 1 and 2 was adopted. Two different materials were used for the surface of the burner. An 1/8 inch thick sintered bronze material is used for the two outer sections (B and C). To permit sufficient flow of sodium through the center section (A), a more porous honeycomb matrix of stainless steel (1/32 inch mesh size) was used. The body of the burner was made of brass.

For cooling of the surface, 1/8 inch copper tubing was coiled around in the middle section of the burner. This section was also packed with 20 mesh zinc shot to aid in heat transfer and mixing of the gases.

The "nebulizer" portion of a burner from a Perkin-Elmer Model 303 atomic absorption spectrometer was used for introducing the sodium. The burner shown in Figures 1 and 2 was made to fit directly to this nebulizer

which included all the connections required for introducing fuel, air and sodium, which was aspirated into the gas flow.

The burner was mounted to a set of translation stages with micrometers which enabled measurements of movements along three axes to an accuracy of at least 1/2 mm to be made.

3.2 Flow Control System

The flow control system for the burner is shown schematically in Figure 3. Zones A, B and C of the burner are the inner and outer combustion zone and the sheath gas zone, respectively. The flow unit consists of three panels; one for the fuel, one for the air and one for the sheath gas. Each panel has a toggle valve on the inlet, a needle valve, pressure gauge and rotameter (flow meter) with a needle valve. There are separate flow meters for each section of the burner. The fuel flow panel is equipped with flash arrestors in each flow line. The flow meter sizes are chosen to given a stoichio- metric methane/air mixture at a maximum flame speed of around 33 cm/s.

The unit was pressure tested for leaks and calibrated using a wet test meter. Polynomial fits were made to the calibration data. Tables of calculated flow rates in litre/min as a function of flow meter reading are given in Tables 2A-D.

3.3 Line-Reversal Optical System

The optical system used is shown schematically in Figure 4. Lenses L1 and L2 have focal lengths of 100 mm and diameters of 42 mm. Light from the lamp filament (14 mm x 2 mm) is focused through the first lens L1 into the flame with a 3/4 reduction in size. The light then passes through the second lens and is focused onto the slits of a GCA McPherson Model 218 scanning monochromator.

The monochromator is f# 5.3 and has a 0.3 m focal length. The ruled grating area is 53 x 53 mm. Circular apertures of 35 mm, 21.0 mm and 37.5 mm were installed at lens L1, lens L2 and the grating, respectively. The monochromator slits were set at 4 mm (height)and 0.05 mm (width). A narrow band interference filter, centred at 589.0 nm was installed between the exit slit and the photomultiplier to prevent any possible scattered radiation from entering the detector.

The aperture stop of the optical system shown in Figure 4 is lens L2. The image of this aperture stop in the preceding optics (Lens L1) then defines the entrance pupil which is located 93 mm from the lamp and has a diameter of 8.4 mm. This corresponds to an angular aperture of 2.6°. The field stop (the stop (or its image) which subtends the smallest angle at the centre of the entrance pupil) is the entrance slit of the

monochromator and its image in the preceding optics (lenses L1 and L2) defines the entrance window. The entrance window is located at the lamp filament and is a 1:1 image of the slit. Thus a portion of the filament 4 mm high by 0.05 mm wide is imaged into the monochromator.

This optical arrangement was used for both line reversal and secondary standard lamp calibration experiments. Thus radiation from the central 4 mm of the tungsten strip was used and the angular aperture over which light was collected was confined to 2.0°. This corresponds very closely to the conditions over which the primary standard was calibrated (2.5° and 6.0 mm). In the line reversal measurements the optical arrangement ensured that every portion of the flame imaged into the monochromator was trans-illuminated by radiation from the lamp. Thus in equation (10), $\delta A = \delta A_1$ and $\delta\Omega = \delta\Omega_1$.

3.4 Strip Filament Lamp Calibration

The primary radiation standard was a GE 30A/6V lamp calibrated by the Eppley Laboratory. It was supplied with calibrations of brightness temperature (at 655.0 nm and 2,000, 2,200 and 2,400 K) and spectral radiance from 225 nm to 2400 nm. The maximum uncertainties in brightness temperature were ±5 K at 2000 K increasing to ±8 at 2400 K. Because of its high cost and relatively short life, this lamp was used to calibrate secondary lamps (GE 18A/6V) which were used in the experiments.

The primary standard was installed in the optical system shown in Figure 4. The lamp current was set to 38.0 amps for which the spectral radiance at 589.0 nm is 78600 W/cm^3-steradian. The resulting photomultiplier output voltage (V_s) was recorded. The lamp to be calibrated was then installed in place of the primary standard with its filament identically positioned. (Reproduction of the position was done with the aid of crossed He/Ne laser beams). A series of measurements of photomultiplier voltage (V_1) as a function of lamp current was then recorded. If a linear relationship between lamp spectral radiance and photomultiplier output is assumed then the spectral radiance of the secondary standard L_i can be calculated from the expression:

$$L_i = \frac{V_i}{V_S} \times 78600$$

The spectral radiances can then be converted to temperatures using equation (11). The temperatures obtained were fitted to a second order polynomial in lamp current and the equation used to calculate the brightness temperature versus lamp current as shown in Table III. The agreement between the calculated and observed values was ≤ 0.3 % with no systematic variation with current.

A check of the self consistency of the primary standard was made by calculating the brightness temperature at 589.0 nm from the known

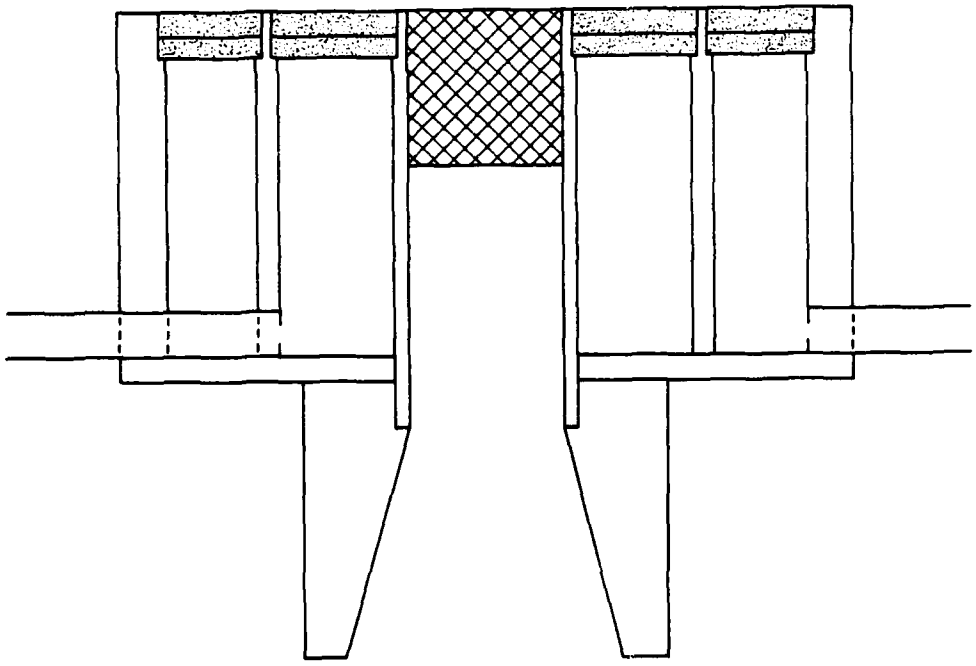

FIGURE 1. BURNER DESIGN

LIST OF FIGURES

TABLE 6

REPRODUCIBILITY OF FLAME TEMPERATURE MEASUREMENTS

T_1	T_2	$\Delta T = T_1 - T_2$	$\Delta T/T_{ave}$%
		PROFILE 1	
2060	2043	17	0.80
2058	2054	4	0.13
2058	2054	4	0.19
2055	2054	1	0.05
2058	2054	9	0.44
2037	2043	6	0.29
2031	2031	0	0.00
2020	2014	6	0.30
2008	1996	12	0.60
		PROFILE 2	
2030	2026	4	0.20
2035	2037	2	0.10
2031	2043	12	0.60
2043	2041	2	0.10
2026	2035	9	0.44
2022	2017	5	0.25
2008	1985	23	1.10
2002	1979	23	1.10
Average of Difference = 0.318%			
Standard Deviation = 0.258%			

TABLE 5

SUMMARY OF EXPERIMENTAL FLAME CONDITIONS

FLAME NO.	EQUIVALENCE RATIO	LINEAR FLOW VELOCITY (COLD) cm/s	LAMINAR FLAME VELOCITY (REF. 5) cm/s	ADIABATIC FLAME TEMPERATURE (REF.6) K	MEASURED CENTRE LINE TEMPERATURE AT N = 4 mm K
1	0.852	24.7	31.5	2068	2028
2	1.001	22.8	41.3	2224	2058
3	1.036	30.0	42.7	2231	2099
4	1.083	29.4	42.3	2220	2081
5	1.179	27.6	40.4	2153	2064
6	1.119	28.4	42.5	2194	2077

TABLE 4

INTERNAL CONSISTENCY CHECK OF PRIMARY LAMP

Lamp Current (Amps)	Measured Temperature (K)	Calibration Temperature (K)	Temperature Difference (K)
37.35	2425	2429	5
32.10	2214	2224	10
27.60	2017	2020	3

The agreement is excellent in general although the 10 K error is somewhat outside the stated accuracy of the brightness temperatures. Of course uncertainty in the radiance value contributes to the temperature error.

TABLE 3. SECONDARY LAMP BRIGHTNESS TEMPERATURE AT 589.0 NM (K) VS LAMP CURRENT (AMPS)

I	0	0.1	0.2	0.3	0.4	0.5	0.6	0.7	0.8	0.9
5	1136.0	1152.3	1168.5	1184.7	1200.7	1216.7	1232.6	1248.5	1264.2	1279.9
6	1295.5	1311.0	1326.5	1341.9	1357.2	1372.2	1387.6	1402.6	1417.6	1432.6
7	1447.4	1462.2	1476.9	1491.5	1506.0	1520.5	1534.9	1549.2	1563.5	1577.6
8	1591.7	1605.7	1619.7	1633.5	1647.3	1661.0	1674.6	1688.2	1701.7	1715.1
9	1728.4	1741.7	1754.8	1767.9	1781.0	1793.9	1806.8	1819.6	1832.3	1845.0
10	1857.5	1870.0	1882.4	1894.8	1907.0	1918.2	1913.3	1943.4	1953.3	1967.2
11	1979.0	1990.8	2002.4	2014.0	2025.5	2036.9	2048.3	2059.5	2070.7	2081.9
12	2082.9	2103.9	2114.8	2125.6	2136.4	2147.0	2157.6	2168.1	2178.6	2188.9
13	2199.2	2209.4	2219.6	2229.6	2239.6	2249.5	2259.4	2269.1	2278.8	2288.4
14	2297.9	2307.4	2316.7	2326.0	2335.3	2344.4	2353.5	2362.5	2371.4	2380.3
15	2389.0	2397.7	2406.3	2414.9	2423.3	2431.7	2440.0	2448.3	2456.4	2464.5
16	2472.5	2480.5	2488.3	2496.1	2503.8	2511.4	2519.0	2526.4	2533.8	2541.2
17	2548.4	2555.6	2562.7	2569.7	2576.7	2583.5	2590.3	2597.0	2603.7	2610.2

TABLE 2 C. FLOW IN LITERS/MIN VS METER READING ZONE A - AIR

	0	1	2	3	4	5	6	7	8	9
10	0.109	0.125	0.142	0.158	0.175	0.191	0.208	0.224	0.241	0.25
20	0.273	0.290	0.306	0.322	0.338	0.354	0.371	0.387	0.403	0.41
30	0.435	0.451	0.467	0.483	0.499	0.515	0.531	0.547	0.562	0.57
40	0.594	0.610	0.626	0.641	0.657	0.673	0.688	0.704	0.719	0.70
50	0.751	0.766	0.781	0.797	0.812	0.828	0.843	0.858	0.874	0.88
60	0.904	0.920	0.935	0.950	0.965	0.980	0.995	1.010	1.025	1.04
70	1.056	1.070	1.085	1.100	1.115	1.130	1.145	1.160	1.175	1.16
80	1.204	1.219	1.233	1.248	1.263	1.277	1.292	1.306	1.32	1.33
90	1.350	1.364	1.379	1.393	1.408	1.422	1.436	1.451	1.465	1.47
100	1.493	1.507	1.522	1.536	1.550	1.564	1.578	1.592	1.606	1.61
110	1.634	1.648	1.662	1.676	1.689	1.703	1.717	1.731	1.745	1.7
120	1.772	1.786	1.799	1.813	1.826	1.840	1.853	1.867	1.880	1.8
130	1.907	1.921	1.934	1.947	1.961	1.974	1.987	2.001	2.014	2.02
140	2.040	2.053	2.066	2.079	2.092	2.105	2.118	2.131	2.144	2.1
150	2.170	2.183	2.196	2.209	2.222	2.234	2.247	2.260	2.272	2.28

TABLE 2 D. FLOW IN LITERS/MIN VS METER READING ZONE B - AIR

	0	1	2	3	4	5	6	7	8	9
10	0.464	0.565	0.666	0.767	0.867	0.968	1.069	1.169	1.269	1.3
20	1.470	1.570	1.669	1.769	1.869	1.968	2.068	2.167	2.266	2.
30	2.464	2.562	2.661	2.760	2.858	2.956	3.054	3.152	3.250	3.3
40	3.446	3.543	3.641	3.738	3.835	3.932	4.029	4.126	4.223	4.3
50	4.416	4.512	4.609	4.705	4.801	4.897	4.992	5.088	5.183	5.2
60	5.374	5.469	5.564	5.569	5.754	5.849	5.943	6.038	6.132	6.2
70	6.320	6.414	6.508	6.602	6.695	6.789	6.882	6.975	7.069	7.1
80	7.254	7.347	7.440	7.532	7.625	7.717	7.809	7.901	7.993	8.0
90	8.177	8.268	8.360	8.451	8.542	8.633	8.724	8.815	8.906	8.9
100	9.087	9.177	9.268	9.358	9.448	9.538	9.627	9.717	9.717	9.
110	9.985	10.074	10.164	10.252	10.341	10.430	10.519	10.607	10.695	10.7
120	10.872	10.960	11.047	11.135	11.223	11.310	11.398	11.485	11.572	11.8
130	11.746	11.833	11.919	12.006	12.092	12.179	12.265	12.351	12.437	12.5
140	12.608	12.694	12.779	12.865	12.950	13.035	13.120	13.205	13.290	13.3
150	13.459	13.543	13.627	13.712	13.796	13.879	13.963	14.047	14.130	14.2

TABLE 2 A. FLOW IN LITERS/MIN VS METER READING ZONE A- CH_4

	0	1	2	3	4	5	6	7	8	9
10	0.007	0.009	0.001	0.013	0.016	0.018	0.020	0.022	0.024	0.027
20	0.029	0.031	0.034	0.036	0.038	0.041	0.043	0.045	0.048	0.050
30	0.052	0.055	0.057	0.060	0.062	0.065	0.067	0.069	0.072	0.074
40	0.077	0.079	0.082	0.085	0.087	0.090	0.092	0.095	0.097	0.100
50	0.103	0.105	0.108	0.111	0.113	0.116	0.119	0.122	0.124	0.127
60	0.130	0.133	0.135	0.138	0.141	0.144	0.147	0.149	0.152	0.155
70	0.158	0.161	0.164	0.167	0.170	0.173	0.175	0.178	0.181	0.184
80	0.187	0.190	0.193	0.196	0.200	0.203	0.206	0.209	0.212	0.215
90	0.218	0.221	0.224	0.228	0.231	0.234	0.237	0.240	0.243	0.247
100	0.250	0.253	0.256	0.260	0.263	0.266	0.270	0.273	0.276	0.280
110	0.283	0.286	0.290	0.293	0.297	0.300	0.304	0.307	0.310	0.314
120	0.317	0.321	0.324	0.328	0.331	0.335	0.339	0.342	0.346	0.349
130	0.353	0.357	0.360	0.364	0.367	0.371	0.375	0.379	0.382	0.386
140	0.390	0.393	0.397	0.401	0.405	0.408	0.412	0.416	0.420	0.424
150	0.428	0.431	0.435	0.439	0.443	0.447	0.451	0.453	0.459	0.463

TABLE 2 B. FLOW IN LITERS/MIN VS METER READING ZONE B - CH_4

	0	1	2	3	4	5	6	7	8	9
10	-0.023	-0.009	0.004	0.018	0.031	0.044	0.058	0.071	0.084	0.9
20	0.111	0.124	0.137	0.150	0.163	0.176	0.189	0.202	0.215	0.2
30	0.241	0.254	0.267	0.279	0.292	0.305	0.317	0.330	0.342	0.3
40	0.367	0.380	0.392	0.405	0.417	0.429	0.441	0.454	0.466	0.4
50	0.490	0.502	0.514	0.526	0.538	0.550	0.562	0.574	0.586	0.5
60	0.609	0.621	0.632	0.644	0.656	0.667	0.679	0.690	0.702	0.7
70	0.724	0.736	0.747	0.758	0.769	0.781	0.792	0.803	0.814	0.8
80	0.836	0.847	0.858	0.869	0.880	0.890	0.901	0.912	0.922	0.9
90	0.944	0.954	0.965	0.975	0.986	0.996	1.007	1.017	1.027	1.0
100	1.048	1.058	1.068	1.078	1.089	1.099	1.109	1.119	1.129	1.1
110	1.148	1.158	1.168	1.178	1.187	1.197	1.207	1.216	1.226	1.2
120	1.245	1.255	1.264	1.273	1.283	1.292	1.301	1.311	1.320	1.3
130	1.338	1.347	1.356	1.365	1.374	1.383	1.392	1.401	1.410	1.4
140	1.427	1.436	1.445	1.453	1.462	1.471	1.479	1.488	1.496	1.5
150	1.513	1.521	1.530	1.538	1.546	1.554	1.562	1.571	1.579	1.6

TABLE 1. TEMPERATURE CORRECTION FOR WAVELENGTH (3)

T(K)	λ = 655 nm		λ^1 = 589.0 nm			λ^1 = 766.5 nm		
(W TEMP)	$\varepsilon(\lambda,T)$	$T_B(\lambda)$	$\varepsilon(\lambda^1,T)$	$T_B(\lambda^1)$	$\Delta T_B(\lambda^1)$	$\varepsilon(\lambda^1,T)$	$T_B(\lambda^1)$	$\Delta T_B(\lambda^1)$
1600	0.442	1510	0.449	1520	+ 10	0.427	1492	- 18
1800	0.438	1686	0.445	1699	+ 13	0.424	1663	- 23
2000	0.433	1858	0.442	1875	+ 17	0.420	1831	- 27
2200	0.429	2028	0.439	2048	+ 20	0.417	1996	- 32
2400	0.425	2195	0.436	2219	+ 23	0.414	2157	- 38
2600	0.420	2358	0.432	2386	+ 28	0.410	2314	- 44
2800	0.417	2519	0.429	2552	+ 33	0.407	2469	- 50
3000	0.414	2677	0.426	2715	+ 38	0.404	2620	- 57

REFERENCES

1. J.P. Botha and D.B. Spalding, Proc. Royal Soc., 225A, 71, 1954.

2. R.D. Larrabee, J. Opt. Soc. Amer. 49, 619, 1959.

3. S.A. Self, Stanford University High Temperature Gas Dynamics Laboratory, Memorandum Report # 14, 1980, "On Tungsten Lamps, Pyrometers and Emissivity Corrections in Temperature Measurements".

4. F.D. Findlay, P. Hughes, R. Mueller and D.R. Snelling, DREO Technical Note to be published.

5. G.E. Andrews and D. Bradley, Combustion and Flame, 20, 77 (1973).

6. O.L Gulder, Division of Mechanical Engineering, National Research Council, Private Communication.

7. W. Snelleman, Combustion and Flame 11, 453 (1967).

An additional source of error is uncertainties in the brightness temperature (or radiance) of the reference light source. As discussed this will lead to a temperature uncertainty of ±8 K at 2400 K decreasing to ±5 K at 2000 K and below.

To determine the precision with which measurements could be made, flames were reproduced and temperature profiles recorded on two different days. A typical result is shown in Table 6. Where two spatial profiles of the flame are shown; measurements were taken every millimetre and profile 1 was from +4 mm to -4 mm and profile 2 from + 3 to -4 mm. The temperatures are the same within 1% and, for the center of the flame, within 0.5%. For the flames tested the average difference between two days readings was 0.40 ± 0.34%. This represents an error of ±8K at 2000K. Snelleman (7) has discussed some additional sources of error due to such effects as stray light and flame scattering of radiation and concludes that they produce systematic errors of approximately 2K.

Taking account of all the sources of error we conclude that the measurements are accurate to ±15K at 2000K.

5.0 CONCLUSIONS

A premixed methane/air flat-flame burner was designed and constructed. The burner had a central flame, which could be seeded with sodium, and an annular guard flame to ensure a flat flame temperature profile in the seeded region. An outer annular flow of sheath gas was provided.

The theory and practise of the line-reversal technique for measuring flame temperatures were discussed. The theoretical expression for flame radiance was shown to be greatly simplified in the limit of uniform flame temperatures.

The sodium line-reversal technique was used to measure the temperatures (line-of-sight averages) as a function of height above the burner and distance from the burner centre line for six flames of differing composition and linear flow velocity.

The burner produced well behaved flat-flames for linear gas velocities of 20-30 cm/s and air to fuel ratios within 15% of stoichiometric. The temperature profiles exhibited a somewhat skewed "top-hat" profile with the temperatures falling-off towards the edge of the flame. The most uniform flame was one with a flame velocity of 30 cm/s consisting of 9.8% methane in air. The temperature 3 mm above the surface on the centre line of this burner was 2095 K.

The sources of error in the sodium line-reversal temperature measurements were examined and it was concluded that the measurements were accurate to ±15 K. The calibration accuracy is more than sufficient to use this burner as a calibration tool in the development of CARS (Coherent anti-Stokes Raman spectroscopy).

Figure 6 that the temperature is still increasing at a height of 4 mm. (Temperature measurements were constrained to 4 mm or less by mechanical considerations.) The vertical flame temperature profile shown in Figure 8 supports this conclusion. (This latter measurement was taken with an optical system in which the height measurements were not constrained in 4 mm or less (4).)

Changes in air/fuel ratio and flame speed do not greatly change the temperatures. A comparison of the results for flame numbers 2 and 3 indicate that a higher temperature flame is associated with a higher flow velocity. This is to be expected since in the higher linear flow velocity flame there will be less heat transfer to the burner required to stabilize the flame.

The most uniform of all the flames recorded was one with a mixture consisting of 9.8% methane and with a flame speed of approximately 30 cm/s. The maximum temperature change for this flame is 50 K. The profile is shown in Figure 6c.

The temperature profiles all show a drop in temperature towards the edge of the centre portion of flame. This may result from the greater cooling encountered by gas flowing close to the cooled center tube. The discontinuity associated with the center tube as the gas emerges from the burner surface and the effect of frictional forces on this gas flow may further contribute to decreases in temperature.

The asymmetry in the profiles shown in Figure 6 is more difficult to understand.

One possible explanation for this is the effect of the 90° bend in the gas flow path just before it reaches the flame (Figure 2). Typically, the velocity profile of the fluid does not return to its uniform state until two diameters downstream from a 90° bend. In the burner set-up used, the diameter of the section at the bend is about one inch and the burner surface is only about 3/4 inches from the bend. A second possible explanation is non-uniform porosity of the sintered metal disc in zone B. The side of the burner giving lower temperatures developed a blemish with use.

4.2 Sources of Error in Sodium Line-Reversal Measurements

It is shown above that account must be taken of the preflame optical transmission F_2. The standard lamp calibration includes the effect of losses in the quartz window. Thus the only optics to be considered is Lens L1. This was a silicate flint lens (SF8) which was coated with a $\lambda/4$ coat of $Mg F_2$. The reflection losses are $< 0.3\%$ per surface or $< 0.6\%$ total. This will lead to an error of approximately 1K in the assigned temperature.

4.0 DISCUSSION OF RESULTS

4.1 Na Line Reversal Measurement

A number of flames were tested with this burner. It was found that mixtures less than 85% and greater than 115% of stoichiometric did not produce flat flames. Low velocity flames (< 20 cm/s) with adequate sodium seeding (see below) were unobtainable since the air flow was insufficient to operate the nebulizer. For flames with gas flow velocities greater than 30 cm/s difficulties were again experienced. In this case, obtaining a flat flame was difficult. The highly turbulent flow also caused non uniform concentrations of sodium in the flame. This is not surprising since the linear gas flow velocity under these conditions is approaching the laminar flame velocity for methane air mixtures (Table 5) and the flame is close to "lifting-off" the burner.

High gas flows also seemed to increase the influence of edge effects. At moderately high flow rates (28-30 cm/s) it was found that a flat flame could not be obtained in zone B of the flame whereas it could in zone A. Since the flame in zone B is there to avoid temperature gradients at the edge of the center flame, it was decided that nonuniformities in this flame would not significantly affect the profile of the center flame.

The temeperature profiles of five methane air flames are shown in Figures 6A-E. The height of the center of the optic axis above the burner (h) in millimeters is shown for each of the curves. The profiles were obtained by moving the burner laterally (with respect to the optical axis) ±5 mm from the center line. This represents a scan across the width of the central zone (A). The composition and linear flow velocity (cold) are shown for zones A and B in Figure 6. Photographs of these flames are shown in Figure 7.

Figure 8 shows a vertical scan (4) of a flame taken with the Na line reversal optical axis on the burner center line. These measurements were performed at a later date than those in Figure 6 with a slightly different optical arrangement (4). A summary of the experimental flame results is given in Table 5.

In one case (Flame 5) the flame front in zone A was higher than for zone B. The difference in height was only a fraction of a millimeter and did not seem to noticeably affect the temperature profile (Figure 6e).

Some general conclusions can be drawn from the profiles shown in Figure 6. The temperatures are lower on one side of the seeded flame by approximately 40K and the average maximum temperature change is 50-60K. The temperature is constant over a 3 to 4 mm horizontal section of the flame particularly on the high temperature side of the flame.

As the measurement height above the burner is increased from 2 to 4 mm the temperature increases by 30-40K. (It should be noted here that a 3 mm vertical section of the flame is being probed. Thus a measurement centred at 3 mm represents an average from 1½ to 4½ mm.) It is clear from

radiance using equation 11 and comparing this to the calibrated brightness temperature. The measured and calibrated brightness temperatures at 589.0 nm are shown in Table 4. The data in Table 1 was used to correct the calibrated values at 655.0 nm to 589.0 nm.

3.5 Sodium Line Reversal Measurements

The desired flame was obtained by adjusting the flow control rotameters. A hand held programmable calculator was used to check the fuel mixtures. Inputs to the program were the desired percent fuel and linear flow speed. Outputs were the flows in liters per minute of both gas and air for both sections of the burner and, finally, the flow of sheath gas through zone C. The composition and linear flow velocity of regions A and B were matched as closely as possible.

The cooling water was turned on and the meter needle valve adjusted to give a constant flow. The flow was such that there was no sensible heating of the water as it passed through the burner. Meter readings for specific gas flows were obtained from the rotameter calibration tables (Tables 2A-D).

With the flame lit, the feed tube of the nebulizer was inserted into a 10% solution of NaOH. The adjustment screw on the nebulizer was set to give the maximum amount of sodium in the flame. The amount was determined visually by the brightness of the flame. The flame was left to burn for five to ten minutes before measurements were taken. The burner mounts were adjusted to position the burner in the desired horizontal and vertical positions.

The calibrated lamp was then turned on and set to some arbitrary current between 9 and 12 amps. The output of the photo multiplier was connected to a strip chart recorder which was operated at a speed of 1 inch/minute.

With the slits set to 50 μm wide by 4 mm high and the wavelength selector at the 587.5 nm the monochromator was scanned at a speed of 5.0 nm/min. A scan was recorded through the wavelength 589.0 nm. (Scanning was only done in one direction.) Depending on the output, the lamp current was increased or decreased and the scan repeated. This was repeated until a temperature match was achieved (i.e. until the two sodium emission lines are invisible against the strip-filament radiation). A typical scan is shown in Figure 5.

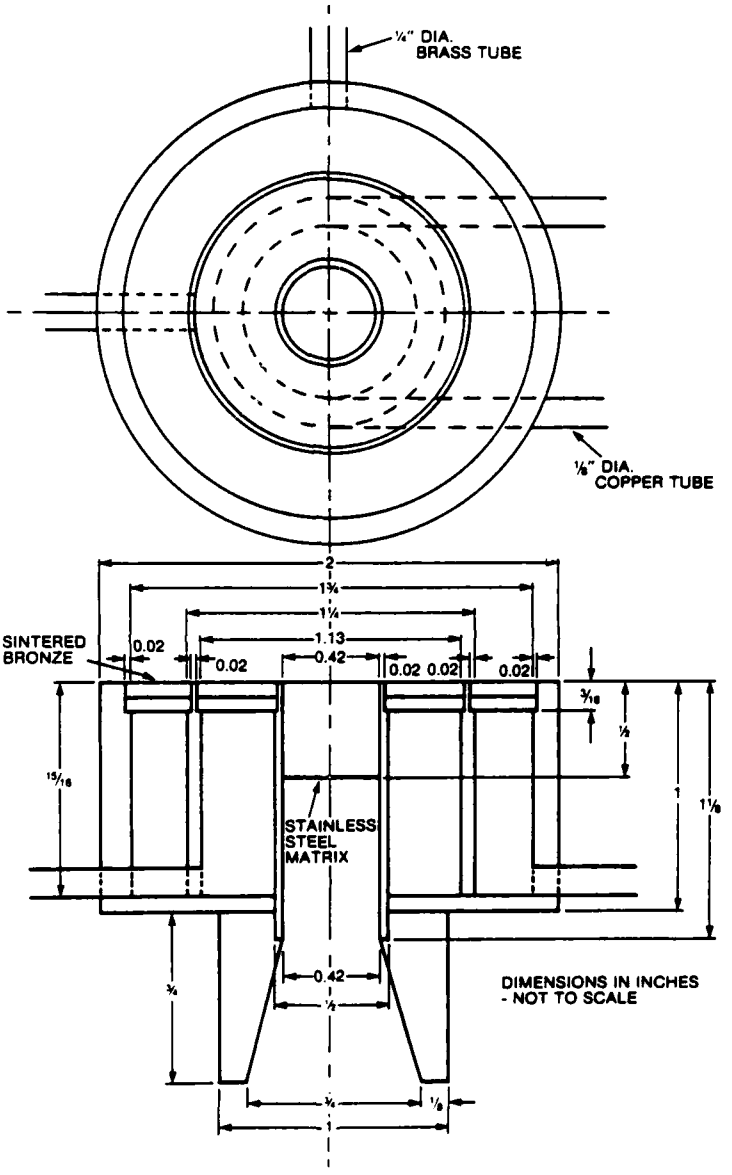

FIGURE 2. FLAT FLAME BURNER CONSTRUCTION

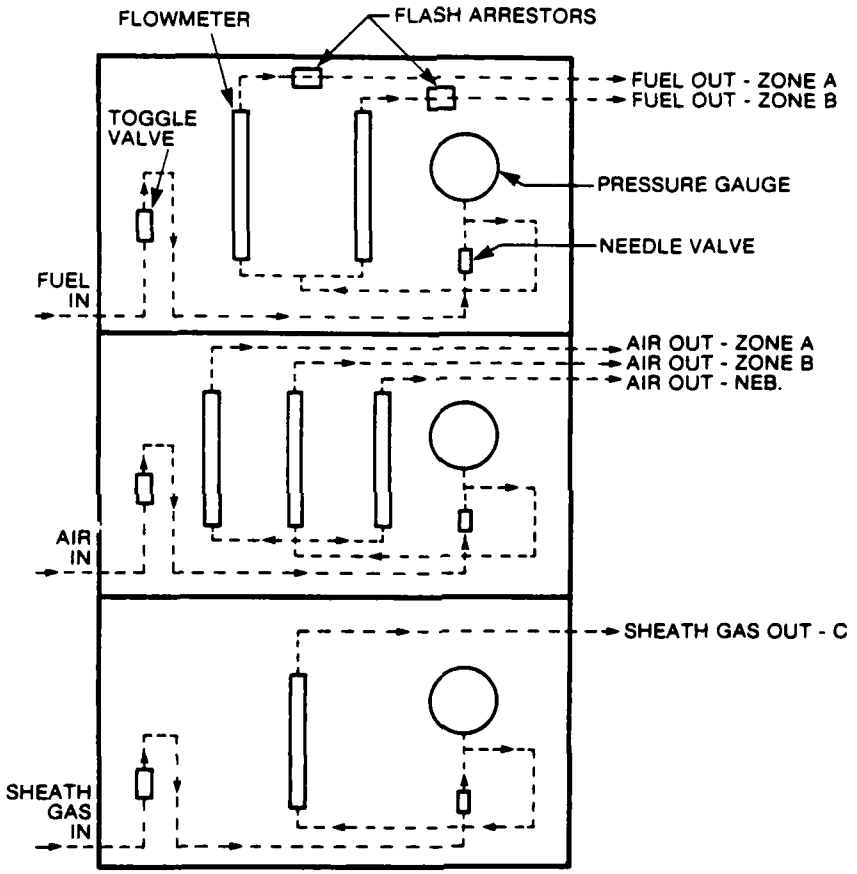

FIGURE 3. SCHEMATIC OF FLOW CONTROL SYSTEM

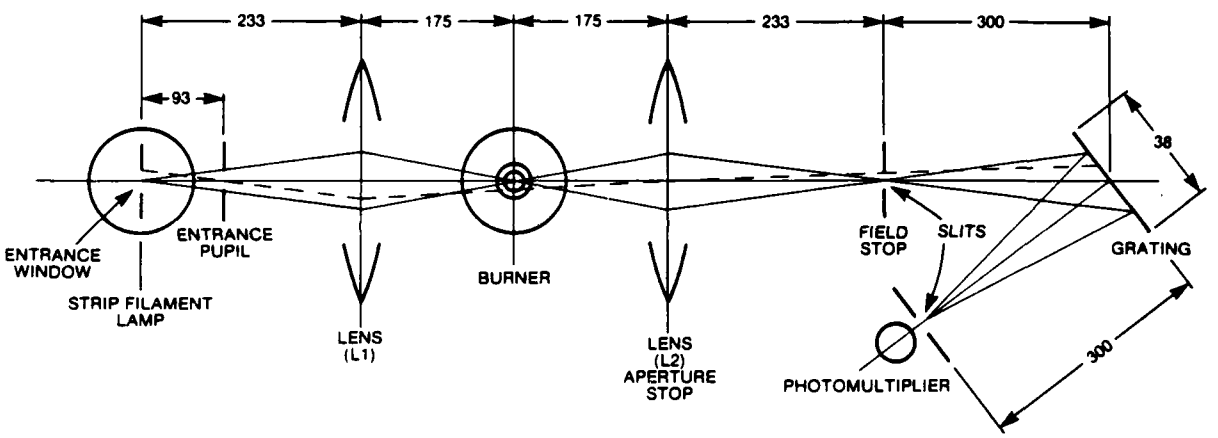

FIGURE 4. OPTICAL SYSTEM FOR Na LINE REVERSAL

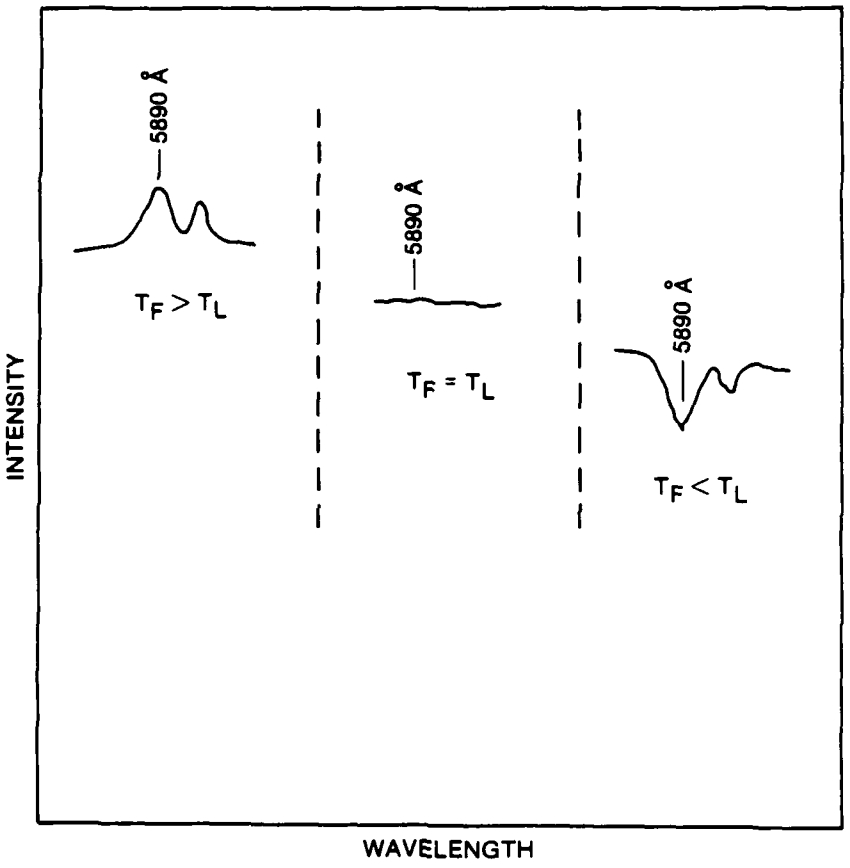

FIGURE 5. SCHEMATIC OF SODIUM LINE REVERSAL SCANS

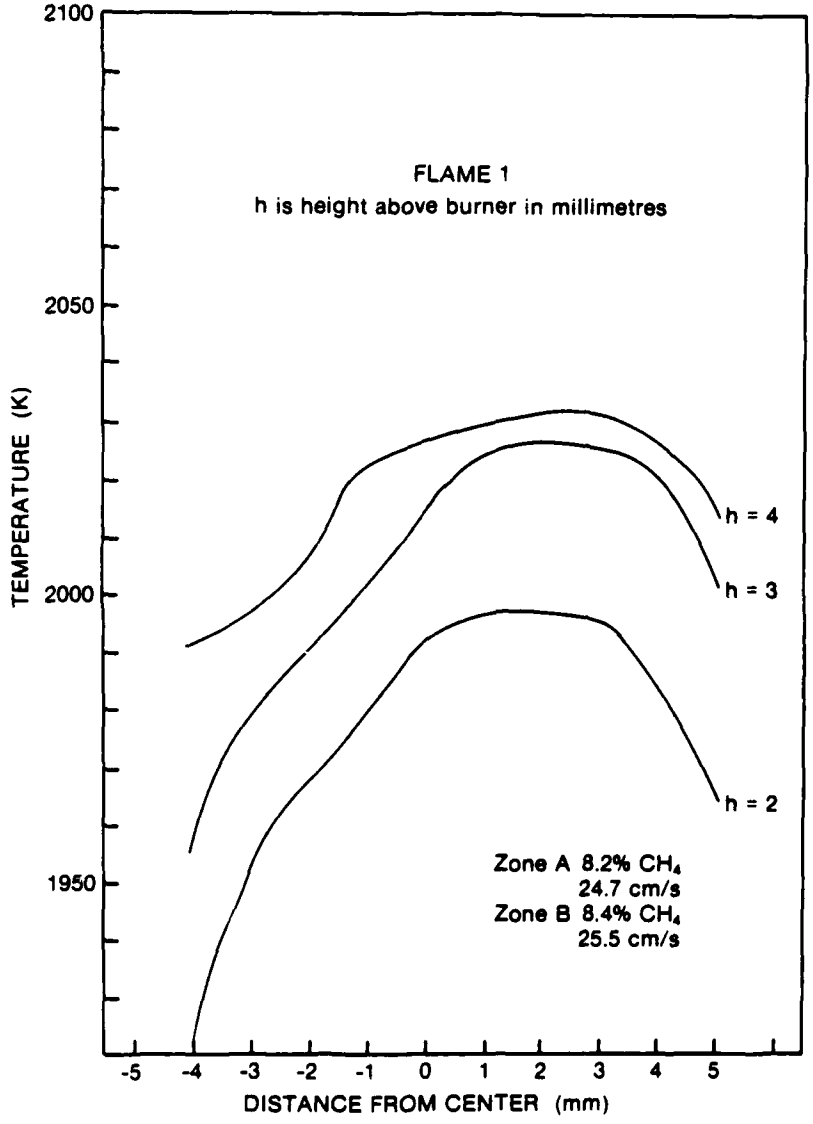

FIGURE 6A. SODIUM LINE REVERSAL TEMPERATURE PROFILES FOR FLAME #1

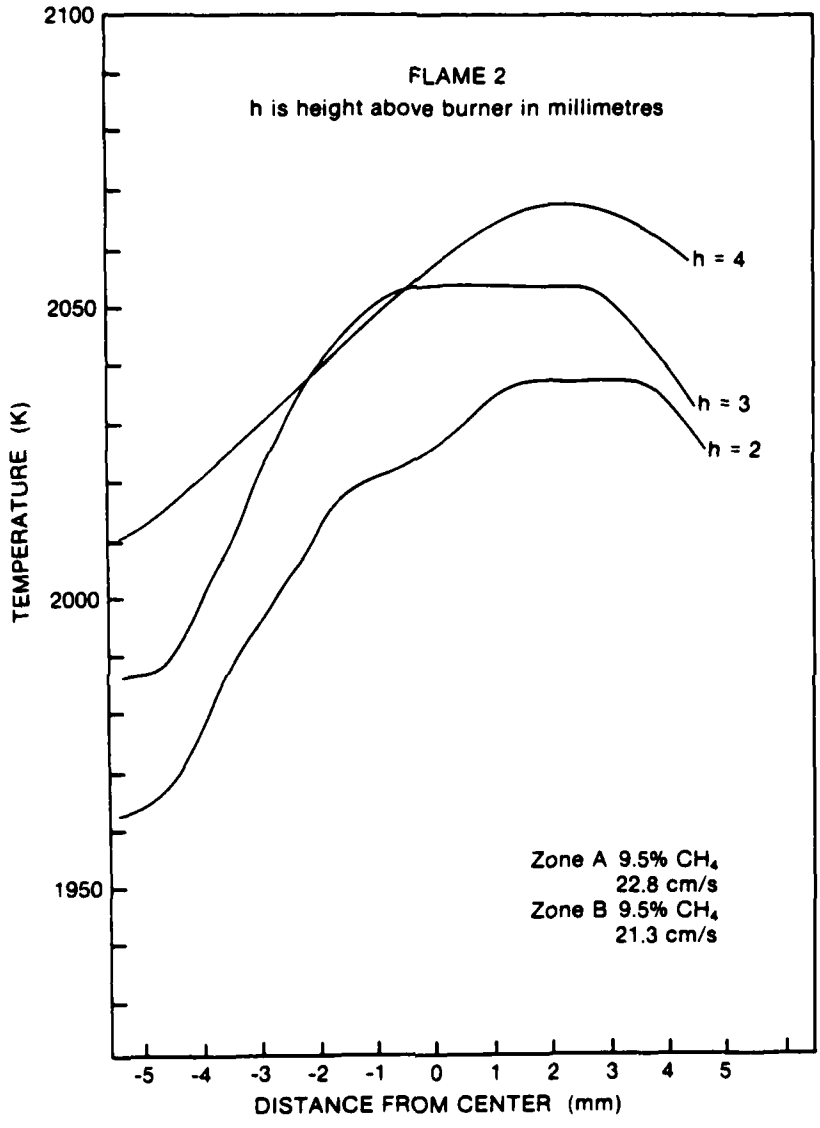

FIGURE 6B. SODIUM LINE REVERSAL TEMPERATURE PROFILES FOR FLAME #2

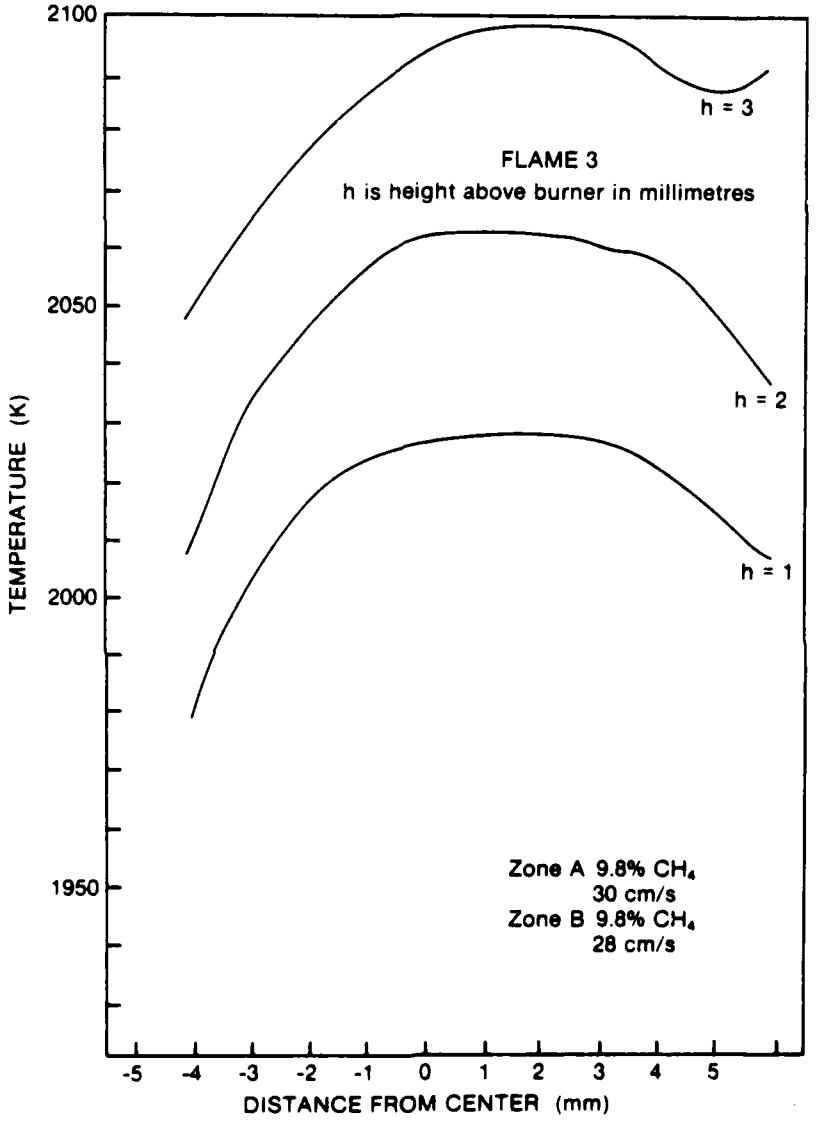

FIGURE 6C. SODIUM LINE REVERSAL TEMPERATURE PROFILES FOR FLAME #3

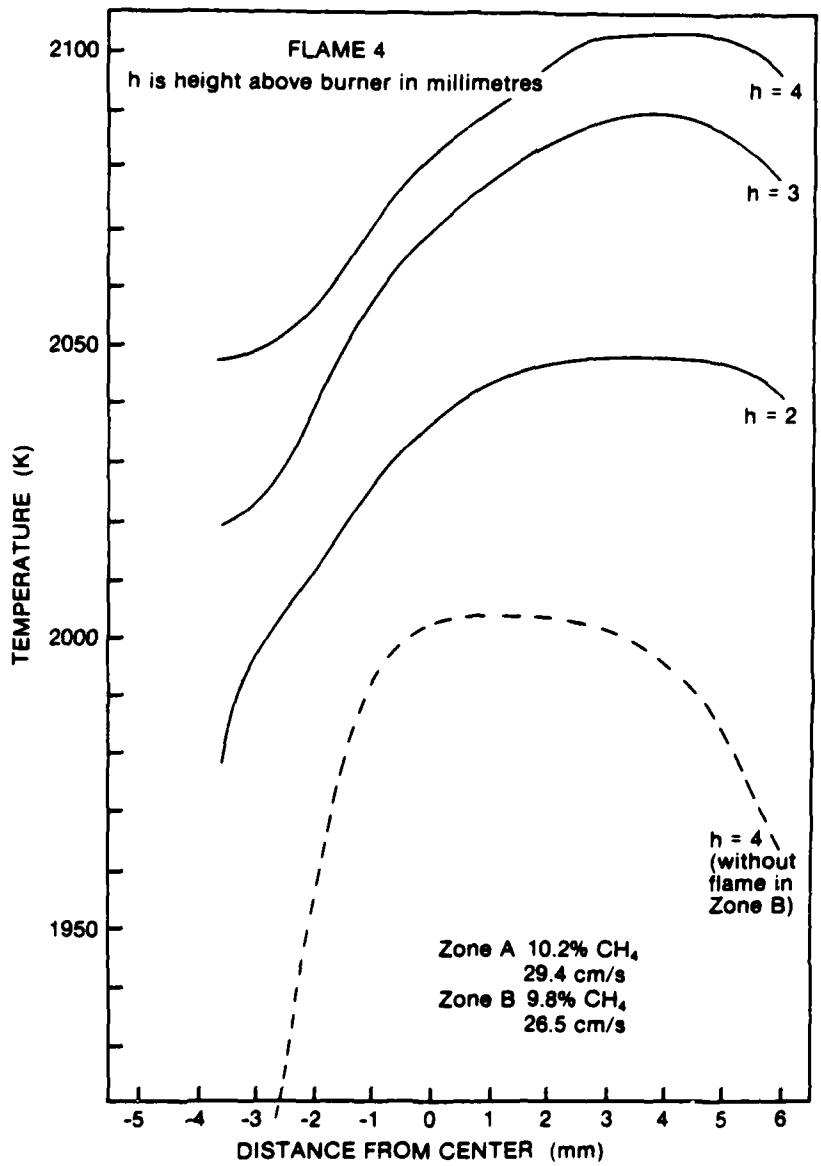

FIGURE 6D. SODIUM LINE REVERSAL TEMPERATURE PROFILES FOR FLAME #4

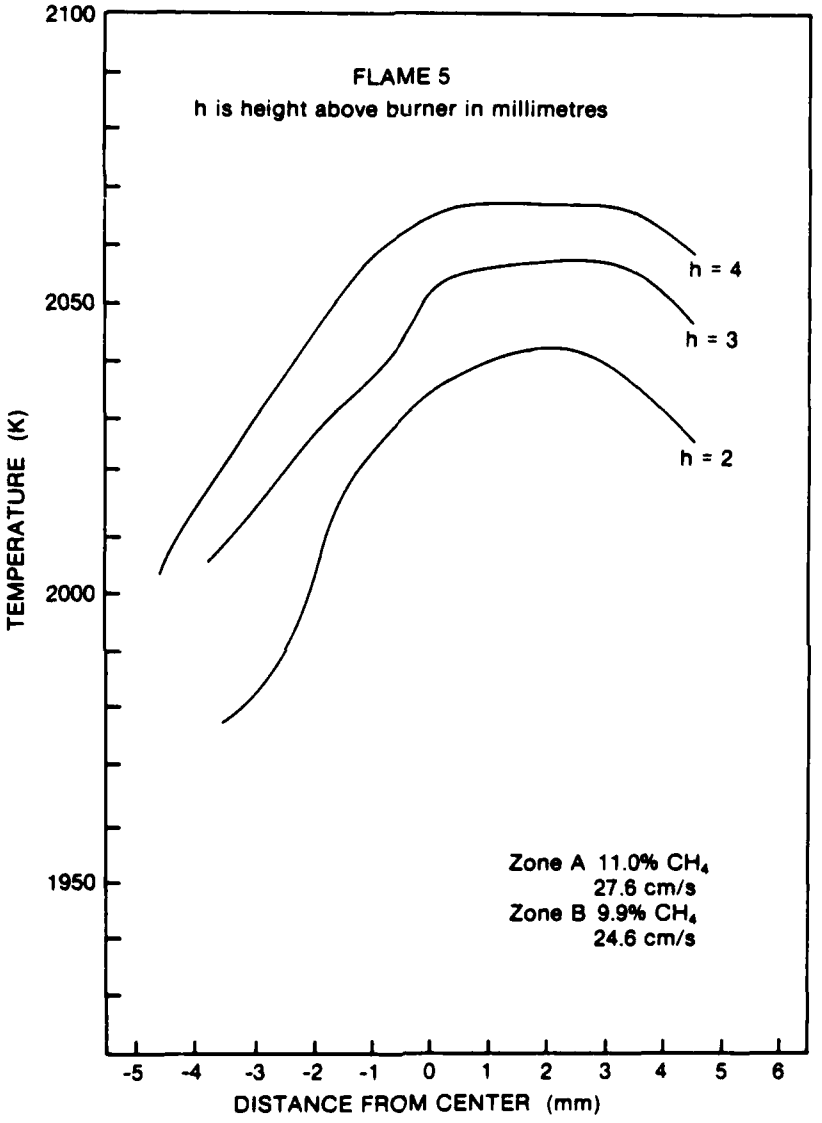

FIGURE 6E. SODIUM LINE REVERSAL TEMPERATURE PROFILES FOR FLAME #5

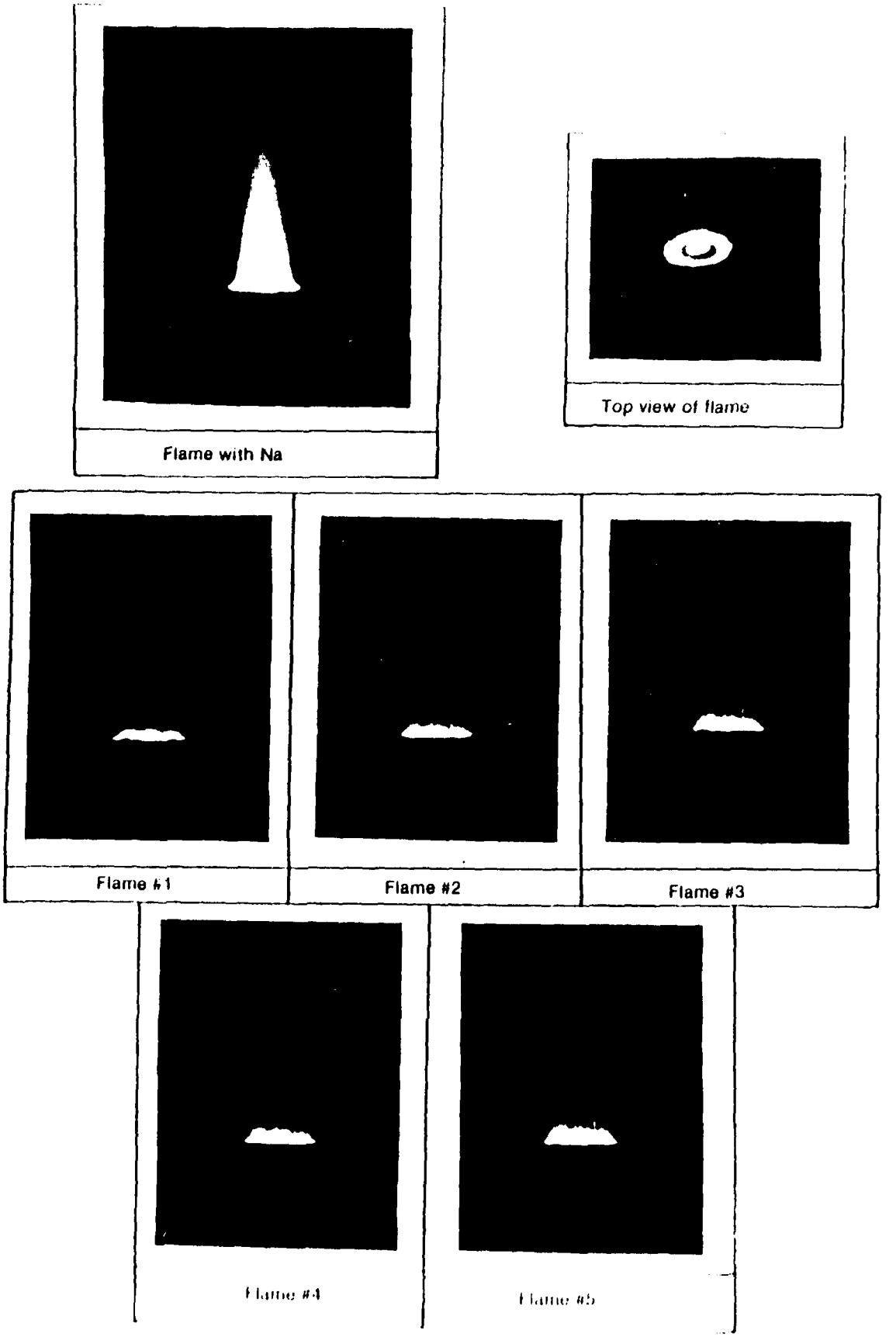

FIGURE 7. PHOTOGRAPHS OF FLAMES

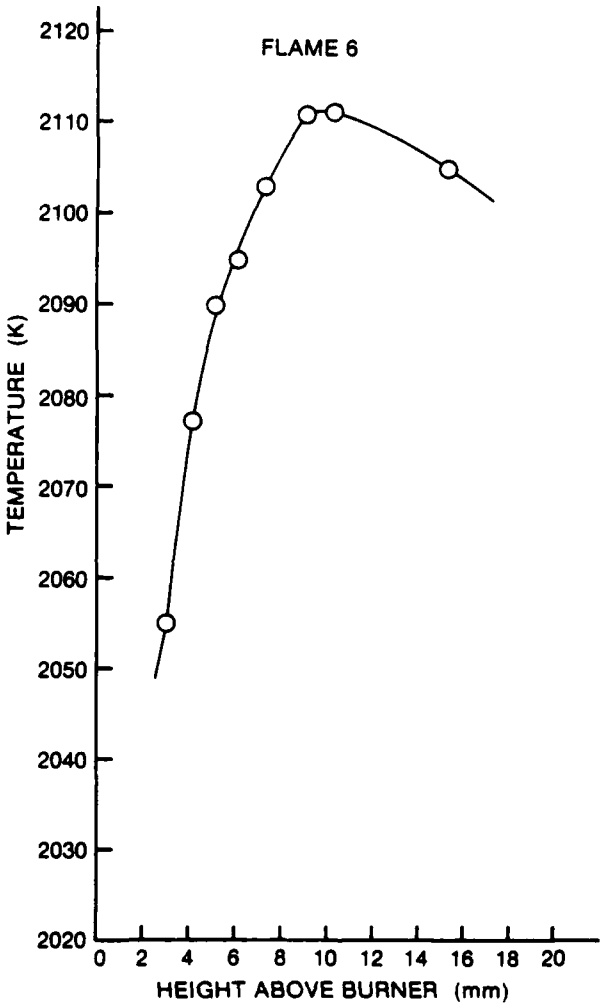

FIGURE 8. SODIUM LINE REVERSAL TEMPERATURE PROFILES FOR FLAME #6

UNCLASSIFIED
Security Classification

DOCUMENT CONTROL DATA - R & D
(Security classification of title, body of abstract and indexing annotation must be entered when the overall document is classified)

1 ORIGINATING ACTIVITY Defence Research Establishment Ottawa Department of National Defence Ottawa, Ontario, K1A 0Z4, Canada	2a. DOCUMENT SECURITY CLASSIFICATION Unclassified 2b GROUP

3. DOCUMENT TITLE

DESIGN AND CALIBRATION OF A FLAT-FLAME BURNER USING LINE REVERSAL TECHNIQUES (U)

4 DESCRIPTIVE NOTES (Type of report and inclusive dates)

5 AUTHOR(S) (Last name, first name, middle initial)

Snelling, D.R. and Fischer, M.

6 DOCUMENT DATE April 1985	7a TOTAL NO OF PAGES 38	7b NO OF REFS 7
8a PROJECT OR GRANT NO 25B10	9a ORIGINATOR'S DOCUMENT NUMBER(S) DREO TN 85-4	
8b CONTRACT NO	9b OTHER DOCUMENT NO (S) (Any other numbers that may be assigned this document)	

10 DISTRIBUTION STATEMENT

Unlimited Distribution

11 SUPPLEMENTARY NOTES	12. SPONSORING ACTIVITY Defence Research Establishment Ottawa

13 ABSTRACT

A premixed methane/air flat-flame burner is described. The burner was designed to have a central flame which could be seeded with sodium, and an annular guard flame which ensured a flat temperature profile in the seeded region.

The burner produced a well behaved flat flame for linear gas velocities of 20 to 30 cm/s and air to fuel ratios within 15% of stoichiometric. The temperature distribution in the flame was measured for a range of operating conditions using the sodium line-reversal technique. The temperatures measured were within the range 2000 - 2100 K, slightly lower than the adiabatic methane/air flame temperature. This burner will be used as a calibration tool in the development of CARS (Coherent anti-Stokes Raman spectroscopy).

DSIS

UNCLASSIFIED

Security Classification

KEY WORDS

Flat-Flame
Burner
Sodium Line Reversal
Temperature
CARS

INSTRUCTIONS

1. ORIGINATING ACTIVITY: Enter the name and address of the organization issuing the document.

2a. DOCUMENT SECURITY CLASSIFICATION: Enter the overall security classification of the document including special warning terms whenever applicable.

2b. GROUP: Enter security reclassification group number. The three groups are defined in Appendix 'M' of the DRB Security Regulations.

3. DOCUMENT TITLE: Enter the complete document title in all capital letters. Titles in all cases should be unclassified. If a sufficiently descriptive title cannot be selected without classification, show title classification with the usual one-capital-letter abbreviation in parentheses immediately following the title.

4. DESCRIPTIVE NOTES: Enter the category of document, e.g. technical report, technical note or technical letter. If appropriate, enter the type of document, e.g. interim, progress, summary, annual or final. Give the inclusive dates when a specific reporting period is covered.

5. AUTHOR(S): Enter the name(s) of author(s) as shown on or in the document. Enter last name, first name, middle initial. If military, show rank. The name of the principal author is an absolute minimum requirement.

6. DOCUMENT DATE: Enter the date (month, year) of Establishment approval for publication of the document.

7a. TOTAL NUMBER OF PAGES: The total page count should follow normal pagination procedures, i.e., enter the number of pages containing information.

7b. NUMBER OF REFERENCES: Enter the total number of references cited in the document.

8a. PROJECT OR GRANT NUMBER: If appropriate, enter the applicable research and development project or grant number under which the document was written.

8b. CONTRACT NUMBER: If appropriate, enter the applicable number under which the document was written.

9a. ORIGINATOR'S DOCUMENT NUMBER(S): Enter the official document number by which the document will be identified and controlled by the originating activity. This number must be unique to this document.

9b. OTHER DOCUMENT NUMBER(S): If the document has been assigned any other document numbers (either by the originator or by the sponsor), also enter this number(s).

10. DISTRIBUTION STATEMENT: Enter any limitations on further dissemination of the document, other than those imposed by security classification, using standard statements such as:

(1) "Qualified requesters may obtain copies of this document from their defence documentation center."

(2) "Announcement and dissemination of this document is not authorized without prior approval from originating activity."

11. SUPPLEMENTARY NOTES: Use for additional explanatory notes.

12. SPONSORING ACTIVITY: Enter the name of the departmental project office or laboratory sponsoring the research and development. Include address.

13. ABSTRACT: Enter an abstract giving a brief and factual summary of the document, even though it may also appear elsewhere in the body of the document itself. It is highly desirable that the abstract of classified documents be unclassified. Each paragraph of the abstract shall end with an indication of the security classification of the information in the paragraph (unless the document itself is unclassified) represented as (TS), (S), (C), (R), or (U).

The length of the abstract should be limited to 20 single-spaced standard typewritten lines; 7½ inches long.

14. KEY WORDS: Key words are technically meaningful terms or short phrases that characterize a document and could be helpful in cataloging the document. Key words should be selected so that no security classification is required. Identifiers, such as equipment model designation, trade name, military project code name, geographic location, may be used as key words but will be followed by an indication of technical context.

END

FILMED

8-85

DTIC